Solid Freeform Fabrication 2018: Proceedings of the 29th Annual International Solid Freeform Fabrication Symposium – An Additive Manufacturing Conference
Reviewed Paper

NUMERICAL PREDICTION OF THE POROSITY OF PARTS FABRICATED WITH FUSED DEPOSITION MODELING

Marcin P. Serdeczny, Raphaël Comminal, David B. Pedersen, Jon Spangenberg

Department of Mechanical Engineering, Technical University of Denmark, Kgs. Lyngby, Denmark

Abstract

In this paper, we study the effect of the printing parameters, namely the layer thickness and the strand-to-strand distance, on the porosity of components produced with Fused Deposition Modeling (FDM). The FDM process is based on the extrusion of a melted material through a nozzle, which forms a 3D object, layer by layer from the subsequent deposition of strands. Previous numerical modeling and experimental studies have showed that the cross-section of the strands depends on the printing parameters. Using computational fluid dynamics simulations, we predict the shape of the cross-sections of multiple strands printed next to each other, and we estimate the porosity of the part. The results of this study show that the porosity of the parts produced by FDM can be controlled by adjusting the printing parameters.

Introduction

Fused Deposition Modeling (FDM) belongs to the family of the extrusion-based additive manufacturing (AM) methods, where a semi-liquid material is selectively deposited along a specified path to create a layered three-dimensional object. The raw material is usually in the form of a thermoplastic filament and is fed to a liquefier that melts it and extrudes it through a nozzle. The extruded strands bond together by means of temperature-driven molecular diffusion [1] and form a rigid porous structure after the solidification. One of the key advantages of the FDM method is a large freedom of geometry that can be manufactured. In addition, extrusion-based AM is cost-effective for a small scale production. The fabricated parts have been mainly employed as prototypes and presentation models but the continuous improvement of the process has enabled a substantial growth of their applications as functional end-use products [2]. Recently, extrusion-based AM was successfully tested on the International Space Station [3].

Despite the large success of the FDM process, there are still many challenges that need to be addressed to ensure its competitiveness. In general, FDM parts have a smaller tensile strength than components fabricated with conventional manufacturing techniques like for instance injection molding [4]. The reduced strength is attributed to the weak inter- and intra-layer bonding and the presence of voids in the final product [5]. A mesostructure with large voids results in a small contact area between the strands and poor bonding. The porosity of fabricated parts is inherent to extrusion-based additive manufacturing and needs to be addressed at the stage of material deposition by choosing appropriately the process conditions [6]. Understanding the development of voids is essential for improving the mechanical strength of the parts, and to enable the production of components with locally controlled properties [7].

The functional relations between the part properties and the process conditions have been a subject to many experimental studies, which are reviewed in [4]. Among many process parameters, the strand-to-strand distance is a crucial for the porosity [6] and the mechanical strength of fabricated parts [8, 9]. The layer thickness and the extrusion flow rate also have an influence on the tensile strength, as they affect the shape of strands and thereby the bonding areas [6, 10]. However, the interplay of the different parameters impedes understanding of the process. As an alternative to empirical studies, numerical modeling has proven to be a useful approach to gain knowledge about the manufacturing processes [11]. Recently, modeling of the FDM using Computational Fluid Dynamics (CFD) has received an increased attention. The temperature distribution within the extruded strands was simulated in [12]. The study was further extended to investigate the thermal stresses and the solidification of the semi-molten material in [13]. The effect of the outer shape of the nozzle on the strand height was presented

in [14]. The influence of the layer thickness and extrusion flow rate on the strand shape and the force exerted on the substrate by the extruded material was reported in [15].

In this work, we show how CFD simulations can be used to gain insight into the development of the mesostructure of FDM parts. By simulating the deposition flow, we predict the morphology of adjacent strands, as well as the porosity they produce. Based on the literature study, we chose to vary the layer thicknesses and the strand-to-strand distance as those are the influential process parameters for the mesostructure of the FDM part. Finally, we estimate the porosities of the simulated specimens and compare the results for the different printing conditions.

Methodology

We simulated the material extrusion in the FDM process using a CFD model implemented in ANSYS Fluent R18.2 [16]. The model assumed an isothermal creeping flow of an incompressible Newtonian fluid, similarly to the work of Comminal et al. (we refer the reader to Ref. [15] for more details about the CFD model and the numerical methods of the simulation). For the simulation of the first strand, the model geometry consisted of a stationary nozzle with the diameter D and a moving substrate with the tangential velocity V (see Figure 1a). For the deposition of the subsequent strands, the volume of the previously extruded material was incorporated to the numerical model as a solid body moving with the same velocity as the substrate (see Figures 1b and 1c). Two layers of four strands each were deposited with the layer thickness t and the strand-to-strand distance s. The strands were extruded in the order shown in Figure 1d. For the first strand, only half of the nozzle geometry was implemented as the flow was symmetrical with respect to the plane cutting through the middle of the nozzle in the direction of the deposition. For the subsequent strands, no symmetrical boundary was applied, and the full domain was resolved (see Figure 1b-c). The material entered the nozzle with the volumetric extrusion flux U. The walls of the nozzle, the substrate and the previously deposited strands were modelled with a no-slip boundary condition. The fluid was free to exit the calculation domain at the outlet boundaries. The density and viscosity of the extruded material were 1000 kg/m^3 and 1000 Pa·s, respectively; however, their actual values did not have an effect on the numerical results, as long as the viscous forces dominated the inertial effects i.e. creeping flow regime, as it is the case in FDM. In such conditions, the material deposition was fully determined by the normalized layer thickness t/D, the velocity ratio V/U, and the normalized strand-to-strand distance s/D. The material deposition was simulated for four sets of printing parameters; see Table 1.

Table 1. Values of the extrusion parameters used in the simulations.

Variable	**Symbol**	**Unit**	**Case 1**	**Case 2**	**Case 3**	**Case 4**
Layer thickness	t	mm	0.32		0.24	
Normalized layer thickness	t/D	-	0.80		0.60	
Strand-to-strand distance	s	mm	0.48	0.4	0.58	0.56
Normalized strand-to-strand distance	s/D	-	1.20	1.0	1.45	1.40
Nozzle diameter	D	mm	0.4			
Extrusion volumetric flux (average velocity inside the nozzle)	U	mm/s	20			
Printing head velocity	V	mm/s	20			
Normalized printing head velocity	V/U	-	1.0			

The governing equations of the fluid flow are the conservation of mass (1) and the conservation of momentum (2):

$$\frac{\partial u_j}{\partial x_j} = 0 \tag{1}$$

$$\rho\left(\frac{\partial u_i}{\partial t}\right) = \frac{\partial p}{\partial x_i} + \mu\frac{\partial^2 u_i}{\partial x_j \partial x_j} + \rho g_i \tag{2}$$

where: u_i is the velocity component in i-direction, x_i is the spatial coordinate, t is the time, ρ is the material density, p is the local pressure, μ is the dynamic viscosity of the fluid, g_i – the component of the gravitational body force per unit mass (non-zero only in the vertical direction), j is the summation index.

The governing equations are solved with the finite-volume method and an implicit temporal discretization. The flows were simulated for 0.6 s, which was enough to reach the steady state solutions. The geometry was discretized using a cut cell method that provided a structured mesh with hexahedral elements. The maximum length of the element edge was globally set to 20 μm but the mesh was locally refined below the nozzle and along the deposition path to 10 μm (see Figure 2). The free surface of the deposited material was tracked with the coupled level-set/volume-of-fluid method.

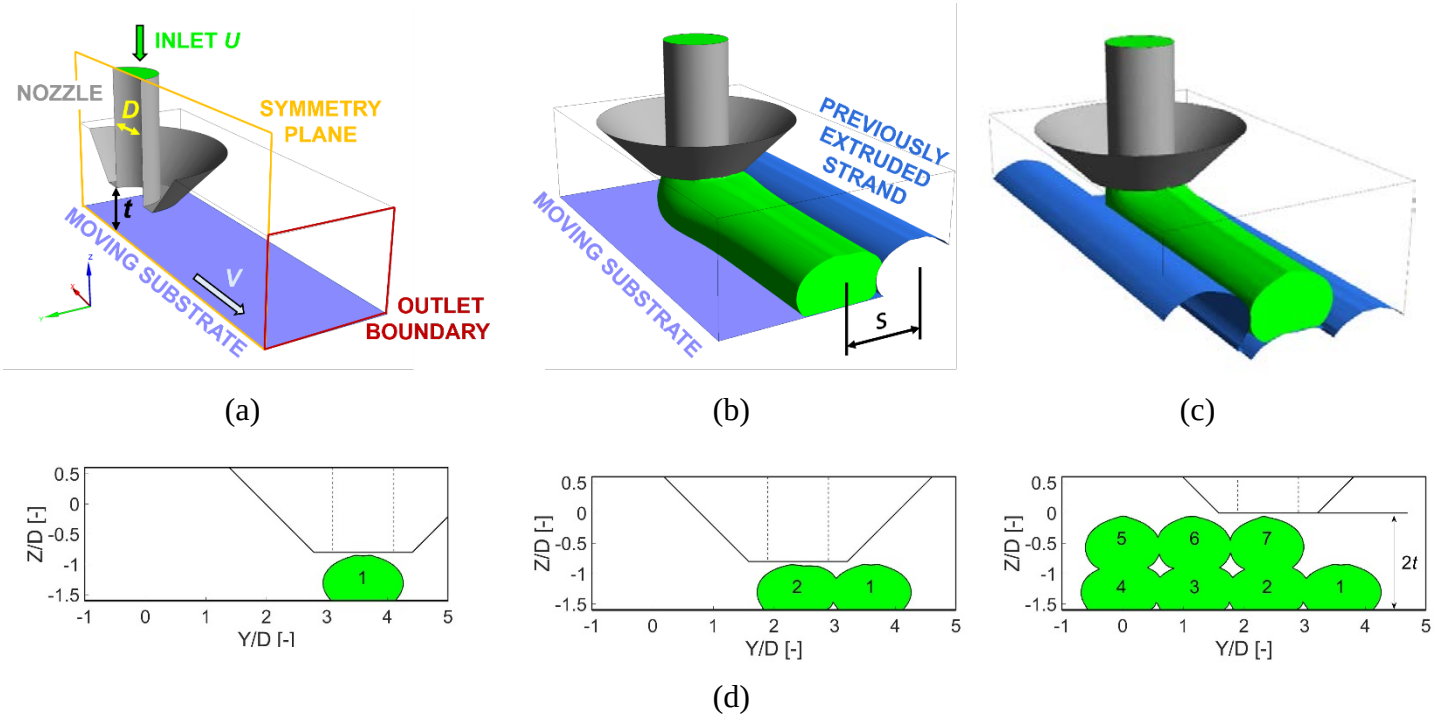

Figure 1. Geometry of the numerical model for the deposition of the first strand (a); the subsequent strands (b, c); and the cross-sections of the strands at the outlet boundary, at the different stages of the deposition process (d). The numbers indicate the order of the deposition. The cross-sectional shape of the first deposited strand was mirrored with respect to the symmetry plane for the sake of visualization.

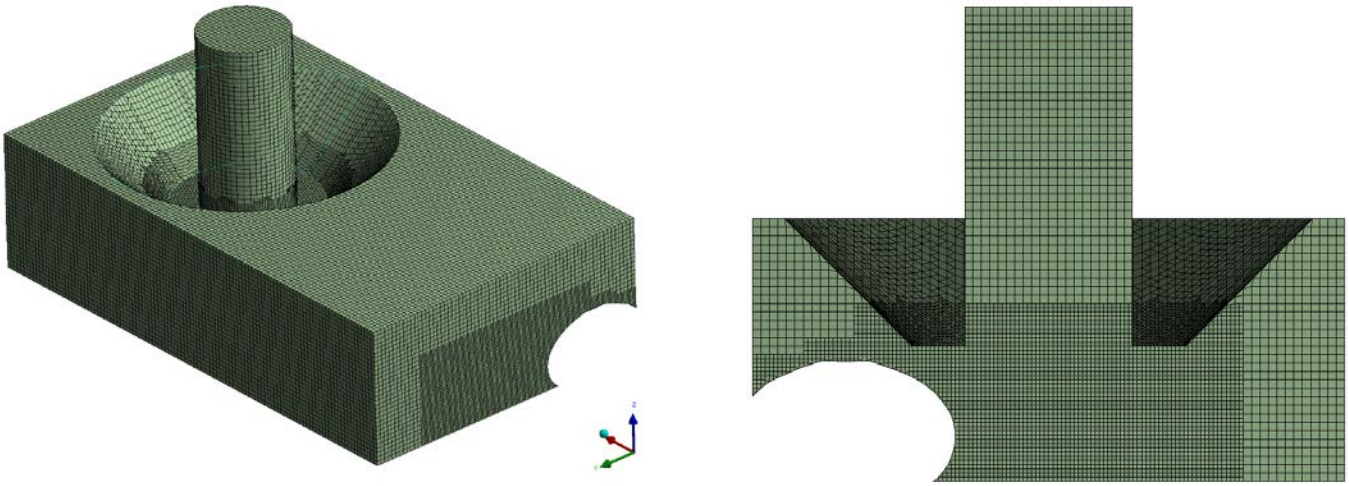

Figure 2. Example of the meshed domain for the simulation of the extrusion of the second strand, for a normalized layer thickness $t/D = 0.8$ and a strand-to-strand distance $s/D = 1.2$.
Isometric view of the entire domain (left), and cross-section through the nozzle (right).

Results and discussions

In this section, the morphology of the strands extruded under the different printing parameters are compared, and the porosity of the printed parts are estimated. Figure 3 shows the predicted mesostructure in the four test cases with different normalized layer thicknesses t/D and strand-to-strand distances s/D. It can be seen that the strands become more cuboid as the layer thickness decreases, while their horizontal contact area with the adjacent layers increases. Moreover, the vertical contact area with the adjacent strands of the same layer increases when the strand-to-strand distance is decreased. The voids between the strands become smaller when both the layer thickness and the strand-to-strand distance are decreased. For the large strand-to-strand distance, the shapes of the strands are regular and repeatable, however for the small strand-to-strand distance, the shapes become distorted and dependent on the order of deposition. For the Case 2 (and to a lesser extend for the Case 4), it is seen that the second layer is shifted horizontally with respect to the first layer. This effect comes from the overlapping of adjacent strands (due to a small strand-to-strand distance) and the fact that the strands of the first and second layers are deposited in reversed order (see Figure 1d). Then, the last strand on each layer is shifted as compared to its nominal position. As it can be seen in Figure 3 (Case 2 and Case 4), these shifts have a negative influence on the surface roughness and the dimensional accuracy of the part.

Table 2 compares the porosity of the printed parts. The porosities were calculated as the area of the void divided by the total area of the rectangular frames shown in Figure 3. The corners of the frames were placed in the middles of the outermost strands. It can be seen that decreasing the layer thickness lowers the porosity, and that further reduction can be achieved by decreasing the strand-to-strand distance.

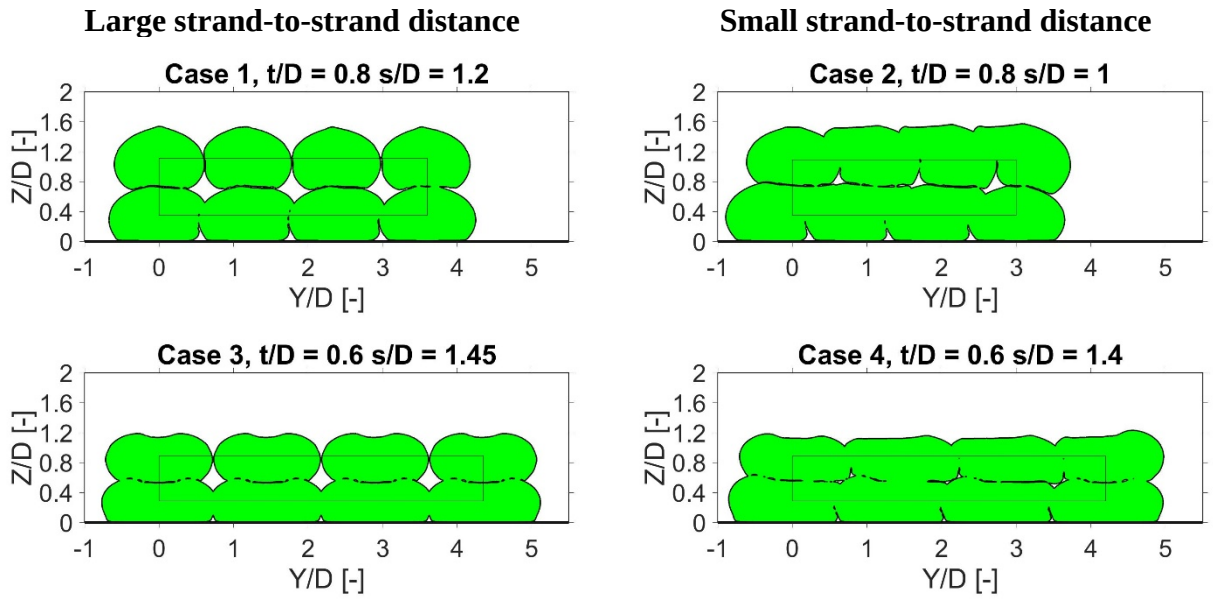

Figure 3. Cross-sections of the simulated strands, extruded at different normalized layer thicknesses *t*/*D* and normalized strand-to-strand distances *s*/*D*. The internal rectangular frames show the representative area used for the calculation of the porosities.

Table 2. Comparison of the porosities for the four cases with different normalized layer thicknesses and strand-to-strand distances.

	Case 1	**Case 2**	**Case 3**	**Case 4**
Normalized layer thickness	0.8	0.8	0.6	0.6
Normalized strand-to-strand distance	1.2	1	1.45	1.4
Porosity	0.100	0.045	0.074	0.015

Conclusions

We have used a three-dimensional numerical model that simulates the isothermal flow of an incompressible Newtonian fluid to investigate the deposition of multiple strands in extrusion-based additive manufacturing. We have predicted the porosity of the specimens that consist of two aligned layers of four strands each. Our results show that both the layer thickness and the strand-to-strand distance have a significant impact on the porosity of the fabricated parts. Among the four test cases that we have inspected, the combination of a normalized layer thickness $t/D = 0.6$ with a normalized strand-to-strand distance $s/D = 1.4$ yielded the most dense packing, with a porosity of 1.5 %. This work shows that CFD simulations can be used to gain insight into the development of the porosity in FDM parts. Further research should extend the present model to simulate the deposition of multiple layers in alternating directions and validate the numerical results with experimental measurements.

Acknowledgments

The authors would like to acknowledge the support of the Danish Council for Independent Research (DFF) | Technology and Production Sciences (FTP) (Contract No. 7017-00128).

References

[1] Q. Sun, G. Rizvi, C. Bellehumeur and P. Gu, "Effect of processing conditions on the bonding quality of FDM polymer filaments", *Rapid Prototyping Journal*, vol. 14, no. 2, pp. 72-80, 2008.

[2] B. N. Turner and S. A. Gold, "A review of melt extrusion additive manufacturing processes: II. Materials, dimensional accuracy, and surface roughness", *Rapid Prototyping Journal*, vol. 21, no. 3, pp. 250-261, 2015.

[3] T. Wohlers, I. Campbell, O. Diegel, J. Kowen and T. Caffrey, "Wohlers Report 2017: 3D Printing and Additive Manufacturing State of the Industry Annual Worldwide Progress Report", Wohlers Associates, 2017.

[4] O. A. Mohamed, S. H. Masood and J. L. Bhowmik, "Optimization of fused deposition modeling process parameters: a review of current research and future prospects", *Advance Manufacturing*, vol. 3, no. 1, pp. 42-53, 2015.

[5] C. Ziemian, M. Sharma and S. Ziemian, "Anisotropic Mechanical Properties of ABS Parts Fabricated by Fused Deposition Modeling", in *Mechanical Engineering*, InTech, 2012.

[6] J. Rodriguez, J. Thomas and J. Renaud, "Characterization of the mesostructure of fused-deposition acrylonitrile-butadiene-styrene materials", *Rapid Prototyping Journal*, vol. 6, no. 3, pp. 175-186, 2000.

[7] L. Li, Q. Sun, C. Bellehumeur and P. Gu, "Composite Modeling and Analysis for Fabrication of FDM Prototypes with Locally Controlled Properties", *Journal of Manufacturing Processes*, vol. 4, no. 2, pp. 129-141, 2002.

[8] K. C. Ang, K. F. Leong, C. Chua and M. Chandrasekaran, "Investigation of the mechanical properties and porosity relationships in fused deposition modelling fabricated porous structures", *Rapid Prototyping Journal*, vol. 12, no. 2, pp. 100-105, 2006.

[9] H. Li, T. Wang and Z. Yu, "The Quantitative Research of Interaction between Key Parameters and the Effects on Mechanical Property in FDM", *Advances in Materials Science and Engineering*, vol. 2017, p. 15 pages, 2017.

[10] J. Chacón, M. Caminero, E. García-Plaza and P. Núñez, "Additive manufacturing of PLA structures using fused deposition modelling: Effect of process parameters on mechanical properties and their optimal selection", *Materials and Design*, vol. 124, no. 15 June 2017, pp. 143-157, 2017.

[11] M. Jabbari, I. Baran, S. Mohanty, R. Comminal, M. Sonne, M. Nielsen, J. Spangenberg and H. J.H., "Multiphysics modelling of manufacturing processes: A review", *Advances in Mechanical Engineering*, vol. 10, no. 5, pp. 1-31, 2018.

[12] H. Xia, J. Lu, S. Dabiri and G. Tryggvason, "Fully Resolved Numerical Simulation of Fused Deposition Modeling. Part I - Fluid Flow", *Rapid Prototyping Journal*, vol. 24, no. 2, pp. 463-476, 2018.

[13] H. Xia, J. Lu and G. Tryggvason, "Fully Resolved Numerical Simulations of Fused Deposition Modeling. Part II. Solidification, Residual Stress, and Modeling of the Nozzle", Preprint arXiv:1711.07094v2, 2017.

[14] J. Liu, K. L. Anderson and N. Sridhar, "Direct Simulation of Polymer Fused Depostion Modeling (FDM) - An implementation of the Multi-Phase Viscoelastic Solver in OpenFOAM", *International Journal of Computational Methods*, vol. 15, no. 1, pp. 1844002:1-19, 2018.

[15] R. Comminal, J. Spangenberg, M. P. Serdeczny and D. B. Pedersen, "Numerical modeling of the strand deposition flow in extrusion-based additive manufacturing", *Additive Manufacturing*, vol. 20, pp. 68-76, 2018.

[16] "ANSYS® FLUENT R18.2, ANSYS FLUENT Theory Guide, © ANSYS, Inc", 2017.